	ESA Climate Change Initiative (CCI)	Page 1
	End-to-end ECV Uncertainty Budget Version 3 (E3UBv3) for the CO <sub>2</sub> _TAN_OCFP version 1.2 product from the University of Leicester	
	for the Essential Climate Variable (ECV) Greenhouse Gases (GHG)	Version 3
		14 <sup>th</sup> February 2022

ESA Climate Change Initiative Plus (CCI+)

# **End-to-end ECV Uncertainty Budget version 3 (E3UBv3) for the University of Leicester Full-Physics XCO<sub>2</sub> TanSat data product (CO<sub>2</sub>\_TAN\_OCFP v1.2)**

—

## **The University of Leicester Full-Physics Retrieval Algorithm for the retrieval of XCO<sub>2</sub> from TanSat**

**for the Essential Climate Variable (ECV)  
Greenhouse Gases (GHG)**

Version 3, revision 1

14<sup>th</sup> February 2022


Written by

Simon Preval, Dongxu Yang, and Hartmut Boesch

Department of Physics and Astronomy, National Centre for Earth Observation, and Space Park Leicester  
University of Leicester


Leicester

United Kingdom

	<b>ESA Climate Change Initiative (CCI)</b> <b>End-to-end ECV Uncertainty Budget Version 3 (E3UBv3) for the CO2_TAN_OCFP version 1.2 product from the University of Leicester</b> <b>for the Essential Climate Variable (ECV) Greenhouse Gases (GHG)</b>	Page 2
		Version 3
		14 <sup>th</sup> February 2022


Document history:

Version	Revision	Date	Description/Comments
1	1	26/10/2019	First version of CO2_TAN_OCFP v1 E3UB document
1	2	20/12/2019	Corrections in response to comments by ESA
2	1	16/12/2020	Update for first global product.
3	0	26/11/2021	First version of CO2_TAN_OCFP v1.1 E3UB document.
3	1	14/02/2022	Updated E3UB document correcting errors in previous CO2_TAN_OCFP v1.1 product, and creation of new product CO2_TAN_OCFP v1.2.

	<b>ESA Climate Change Initiative (CCI)</b> <b>End-to-end ECV Uncertainty Budget Version 3 (E3UBv3) for the CO2_TAN_OCFP version 1.2 product from the University of Leicester</b> <b>for the Essential Climate Variable (ECV) Greenhouse Gases (GHG)</b>	Page 3
		Version 3
		14 <sup>th</sup> February 2022

## Contents

1.	List of tables and figures .....	4
1.1	List of tables .....	4
1.2	List of figures .....	4
2.	Executive Summary .....	5
3.	Introduction .....	6
3.1	Purpose of document .....	6
3.2	Intended audience .....	6
3.3	Error term definitions .....	6
4.	Error sources .....	7
4.1	Systematic error .....	7
4.2	Random error .....	7
5.	Methodology .....	8
5.1	TanSat mission .....	8
5.2	UoL CO2_TAN_OCFP v1 .....	8
5.3	TCCON .....	9
5.4	Co-location .....	9
6.	Error results .....	10
6.1	Overview statistics .....	10
6.2	Systematic error .....	10
6.3	Correlations .....	14
6.4	Random error .....	14
7.	Conclusions .....	16
8.	Acknowledgement .....	17
9.	References .....	17

	<b>ESA Climate Change Initiative (CCI)</b> <b>End-to-end ECV Uncertainty Budget Version 3 (E3UBv3) for the CO2_TAN_OCFP version 1.2 product from the University of Leicester</b> <b>for the Essential Climate Variable (ECV) Greenhouse Gases (GHG)</b>	Page 4
		Version 3
		14 <sup>th</sup> February 2022

## 1. List of tables and figures

### 1.1 List of tables

**Table 1.** Error statistics for all TCCON sites considered for XCO<sub>2</sub> validation. Final row details statistics for all sites, with all co-located points used for calculations. XCO<sub>2</sub> units in ppm. The overall of Mean  $\Delta$  and  $\sigma\Delta$  is calculated by averaging of site value and  $r$  is calculated by all individual measurement. Only TCCON measurements over than 20 during each TanSat overpass has been involved in this validation. .... 10

### 1.2 List of figures

**Figure 1.** Correlation between all 113,120 co-located CO2\_TAN\_OCFP and TCCON XCO<sub>2</sub> pairs coloured by site. .... 11


**Figure 2.** TanSat XCO<sub>2</sub> (CO2\_TAN\_OCFP v1) observations plotted with their corresponding paired TCCON mean for the overpass. Overview statistics for each site reference to Table 1. .... 12

**Figure 3.** Monthly mean OCFP bias against TCCON (all 20 TCCON sites). Vertical error bars represent monthly standard deviation of the bias (the standard deviation of all individual bias). .... 12

**Figure 4.** Overpass mean of each individual TCCON–OCFP  $\Delta$  XCO<sub>2</sub> at 8 TCCON sites. The vertical error bar indicates the standard deviation of individual TCCON–OCFP  $\Delta$  XCO<sub>2</sub>. .... 13


**Figure 5.** XCO<sub>2</sub> bias correlations with total aerosol optical depth, total cirrus optical depth, solar zenith angle (SZA), scale factor of water vapor column and offset of temperature profile (column from left to right) for all co-located TCCON–OCFP pairs. The rows indicate the 9 footprints from top to bottom. The linear regression parameters, slope ( $k$ ) and offset ( $b$ ), is shown in each sub-plot. .... 14

**Figure 6.** Correlation plot of the overpass mean estimate of the a posteriori retrieval error and TCCON–OCFP  $\Delta$  standard deviation for different TCCON sites. Slope and intercept are annotated on plots. .... 15

	<b>ESA Climate Change Initiative (CCI)</b> <b>End-to-end ECV Uncertainty Budget Version 3 (E3UBv3) for the CO2_TAN_OCFP version 1.2 product from the University of Leicester</b> <b>for the Essential Climate Variable (ECV) Greenhouse Gases (GHG)</b>	Page 5
		Version 3
		14 <sup>th</sup> February 2022

## 2. Executive Summary

This report provides a summary of the error characterisation work for the University of Leicester OCFP/TanSat v1.2 XCO<sub>2</sub> product (CO2\_TAN\_OCFP v1.2). CRDP#7 provides global (land-only) nadir data from the entire publically available TanSat catalogue spanning 1<sup>st</sup> March 2017 to 23<sup>rd</sup> May 2018. The E3UB work and validation was originally performed using TanSat overpasses over TCCON sites. CRDP#6 provided global (land-only) nadir data from TanSat for June and August 2017 using the CO2\_TAN\_OCFP v1 product. An error in the bias correction has been corrected in the CRDP#6 product and CO2\_TAN\_OCFP v1.1 has been produced with the correct bias correction applied. An additional error in the assignment of the quality flags in CO2\_TAN\_OCFP v1.1 has been corrected in the CO2\_TAN\_OCFP v1.2. This data product which will be released with CRDP#7. Both corrected errors have not been present in the TanSat data release for TCCON-sites only (CRDP#5) which is used for the validation. Therefore, the validation performed for CRDP#5 is still valid and applies to CRDP#7. The product used for the E3UB is CO2\_TAN\_OCFP v1 (CRDP#5), and will be referred to henceforth in this document. The CO2\_TAN\_OCFP v1 product is validated with co-located Total Column Carbon Observing Network (TCCON) Fourier Transform Spectrometer (FTS) measurements from CRDP#5. High overall correlation between matched soundings of 0.82 is found. Systematic and random errors are 0.19 ppm and 1.78 ppm respectively. Stability has not been assessed due to the short time series. Tests are made for correlations with influential external retrieval parameters.

	<b>ESA Climate Change Initiative (CCI)</b> <b>End-to-end ECV Uncertainty Budget Version 3 (E3UBv3) for the CO<sub>2</sub>_TAN_OCFP version 1.2 product from the University of Leicester</b> <b>for the Essential Climate Variable (ECV) Greenhouse Gases (GHG)</b>	Page 6
		Version 3
		14 <sup>th</sup> February 2022

## 3. Introduction

### 3.1 Purpose of document

This E3UB provides an overview of random and systematic errors affecting the UoL CO<sub>2</sub>\_TAN\_OCFP v1.2 TanSat XCO<sub>2</sub> retrieval submitted for the European Space Agency's Green House Gases Climate Change Initiative plus (ESA GHG-CCI+) Climate Research Data Package version No.5 (CRDP#5) and No. 7 (CRDP#7). CRDP#6 is omitted due to the error described in the executive summary. CRDP#5 uses the UoL CO<sub>2</sub>\_TAN\_OCFP v1 TanSat XCO<sub>2</sub> retrieval while CRDP#7 uses the UoL CO<sub>2</sub>\_TAN\_OCFP v1.2 TanSat retrieval. CRDP#7 uses the same validation performed in CRDP#5. CRDP#5 covers the March 2017 to May 2018 period for overpasses over TCCON sites only, while CRDP#7 includes global (land only) nadir data for 1<sup>st</sup> March 2017 to 23<sup>rd</sup> May 2018.

Application of confidence limits to the retrieval are required to translate remotely sensed data presented here into model estimates of XCO<sub>2</sub> with a known degree of confidence, allowing detection of climate change impacts additional to the natural variability of greenhouse gases. GHG-CCI+ user requirements have placed strict measurement accuracy and precision requirements on participating GHG retrievals, enabling identification of minute changes in magnitude and sign of XCO<sub>2</sub> concentrations /Buchwitz et al., 2011, 2015/.


### 3.2 Intended audience

This document is intended for users in the modelling community applying the CO<sub>2</sub>\_TAN\_OCFP v1.2 product for CO<sub>2</sub> inversions, and remote sensing experts interested in atmospheric soundings of XCO<sub>2</sub>. Work presented here should give users a better understanding of error implicit to this GHG-CCI+ product.

### 3.3 Error term definitions

Error terms used in this report are defined to maintain consistency with other CCI (CCI+) user group error terms recommended at the 2014 CCI co-location meeting. Following the descriptions of /Buchwitz et al., 2015/ and /Wagner et al., 2012/:

Error	Difference between measured values and reality (residual of a measurement's accuracy).
Uncertainty	Degree of confidence in the range of a measured value's truth (standard deviation).
Absolute accuracy	Proximity of remotely sensed measurement to in-situ measurement, assuming the in-situ measurement is able to provide a best estimate of observed quantity. Absolute accuracy reflects the best effort of the remote sensing system at reproducing the real-world value by incorporating all random and systematic errors affecting the retrieval.
Relative accuracy	Ratio between the instrument's calibration standard (the best possible measurement the instrument is able to make) against the instrument characteristics at the time of measurement.
Precision	Repeatability of a measurement.
Stability	Systematic error over time, with random errors largely removed by averaging of observations.
Sensitivity	Change of measurement due to instrumental and algorithmic response to physical or simulated input parameters.

	<b>ESA Climate Change Initiative (CCI)</b> <b>End-to-end ECV Uncertainty Budget Version 3 (E3UBv3) for the CO2_TAN_OCFP version 1.2 product from the University of Leicester</b> <b>for the Essential Climate Variable (ECV) Greenhouse Gases (GHG)</b>	Page 7
		Version 3
		14 <sup>th</sup> February 2022

## 4. Error sources


The majority of error is added to measurements from sources grouped into two themes – scattering of radiation into and out of the sampled light path by poorly quantified aerosol loading, cloud, surface reflectivity and meteorological parameters (temperature, pressure and humidity); and instrumental uncertainties (cross section and solar model inaccuracy, system noise and measurement resolution of instrument components) /Boesch et al., 2011/ /Connor et al., 2008/. In addition to single measurement error, issues of correlation lengths are introduced when the retrievals are used for subsequent generation of Level-3 products /Buchwitz et al., 2015/ /Chevallier et al., 2014/. The aforementioned errors can be further grouped into systematic – those which remain stable across measurement series; and random error components – noise in the system induced by unexpected and / or unaccounted for stimuli.

### 4.1 Systematic error

Systematic retrieval errors include algorithmic effects such as inaccuracy in the solar and radiative transfer models, essentially static for the duration of a satellite instrument's operation. The same applies to restrictions in instrument calibration accuracy, for instance modelling of the instrument line shape, which remains fixed following launch (although is modifiable when enough information on ILS degradation is accrued to model degradation effects). Viewing geometry also affects retrievals in a regular fashion by modifying the light path of sensed radiation as a function of the instrument and Sun's position, however interplay between increased path lengths and random error components such as aerosol optical depth add complications to the issue of measurement geometry. A-priori error added to XCO<sub>2</sub> measurements occurs when the retrieval ingests inaccurate input data from models and databases of surface reflectivity, surface pressure, vertical pressure grids, humidity profiles and a-priori CO<sub>2</sub> profiles.

### 4.2 Random error

Random errors are introduced to observations at the sensing stage of a measurement by detector noise, although to a certain extent this error parameter can be estimated as a function of detector component signal to noise ratios during instrument calibration. Far more significantly, atmospheric parameters are able to have major effects on sounding measurements by scattering light in and out of the sensed column. Errors due to unknown aerosol parameters are particularly pronounced where the scattering and absorption effects of suspended particulate matter are poorly modelled, as they inevitably will be when accounting for a tiny subset of all aerosol sizes, morphology and composition. Scattering due to high, optically thin clouds that are not screened from observation record present similar problems.

	<b>ESA Climate Change Initiative (CCI)</b> <b>End-to-end ECV Uncertainty Budget Version 3 (E3UBv3) for the CO<sub>2</sub>_TAN_OCFP version 1.2 product from the University of Leicester</b> <b>for the Essential Climate Variable (ECV) Greenhouse Gases (GHG)</b>	Page 8
		Version 3
		14 <sup>th</sup> February 2022

## 5. Methodology

### 5.1 TanSat mission

The Chinese Global Carbon Dioxide Monitoring Scientific Experimental Satellite (TanSat) is the first Chinese CO<sub>2</sub> monitoring satellite /Chen et al., 2012/, launched on 22nd December 2016. TanSat provides global measurements of total column CO<sub>2</sub> from its NIR/SWIR bands. The mission aims are to monitor the column density of CO<sub>2</sub> precisely and frequently worldwide, to study the absorption and emission levels of CO<sub>2</sub> on a regional scale over a certain period of time, and to develop and establish advanced technologies that are essential for precise CO<sub>2</sub> observations /Liu et al., 2018/.

As the primary instrument onboard TanSat, Atmospheric Carbon dioxide Grating Spectrometer (ACGS) is designed to measure NIR/SWIR backscattered sunlight in the molecular oxygen (O<sub>2</sub>) A band (0.76 µm) and two CO<sub>2</sub> bands (1.61 and 2.06 µm). Total column CO<sub>2</sub> is mainly determined from measurements of its absorption lines in the weak band (1.61 µm). Sunlight is significantly scattered and absorbed by air molecules and suspended particles (e.g., clouds and aerosols), which would result in serious errors in CO<sub>2</sub> retrievals. Consequently, more information from cloud and aerosol measurements is required for the CO<sub>2</sub> retrieval to correct the light path. This is acquired by the O<sub>2</sub> A band that provides information on altitude and total amount (optical depth) of aerosols and clouds due to almost constant and stable O<sub>2</sub> concentrations in the atmosphere. In comparison, the interference from water vapour absorption is relatively weak. However, the CO<sub>2</sub> weak band is spectrally far away from the O<sub>2</sub> A band, and aerosol and cloud optical properties depend on wavelength. Thus, it is also necessary to constrain this spectral variation which is one of the purposes of the strong CO<sub>2</sub> band. The strong CO<sub>2</sub> band also provides information on water vapour and temperature, which reduces impacts from uncertainties in these parameters.


The design of the optical layout of ACGS and the specifications of instrument optical parameters can be found in a previous study /Lin et al., 2017/. The footprint on the ground is 2 km × 2 km in the nadir mode with 9 footprints in each swath and a total width of the field of view (FOV) of ~18 km at nadir. The first global carbon dioxide maps produced from TanSat measurements have been produced by IAPCAS (Institute of Atmospheric Physics Carbon dioxide retrieval Algorithm for Satellite remote sensing) TanSat algorithm /Yang et al., 2018/, and then verified (~2.11 ppm of precision in 8 TCCON sites average) by TCCON Total Carbon Column Observing Network measurements /Liu et al., 2018/.

### 5.2 UoL CO<sub>2</sub>\_TAN\_OCFP v1

The UoL core CO<sub>2</sub> ECV product is retrieved from calibrated TanSat SWIR/NIR spectra using the UoL full-physics retrieval algorithm /Boesch et al., 2011/. The retrieval algorithm obtains XCO<sub>2</sub> in parts per million from a simultaneous fit of the near-infrared O<sub>2</sub> A band spectrum at 0.76 µm and the CO<sub>2</sub> band at 1.61 µm as measured by the TanSat instrument.

The retrieval algorithm employs an iterative retrieval scheme based on Bayesian optimal estimation to estimate a set of atmospheric, surface and instrument parameters from measured spectral radiances. The forward model consists of coupled radiative transfer (RT) and solar spectrum models, calculating the monochromatic spectrum of light originating from the Sun, passing through the atmosphere, reflecting from Earth's surface or scattering back from the atmosphere, exiting at the top of the atmosphere (TOA) and entering the instrument. TOA radiances are then passed to the instrument model to simulate measured radiances at the appropriate spectral resolution. The forward model employs the LIDORT RT model combined with a fast 2-orders-of-scattering vector radiative transfer code /Natraj et al., 2008/. Additionally, the code uses low-stream interpolation functionality /O'Dell, 2010/ to accelerate the RT component of the retrieval algorithm. The OCFP algorithm retrieves a CO<sub>2</sub> profile together with a number of additional parameters including scaling factors for H<sub>2</sub>O and temperature profile, surface pressure, surface albedo, Solar-Induced chlorophyll Fluorescence (SIF, zero offset) and spectral slope per band, spectral shift and stretch / squeeze, extinction profiles of two aerosol profiles and one cirrus cloud profile. In addition, a wavelength dependence gain scale factor has been retrieved as an eight-orders Fourier series (See detail in Algorithm Theoretical Basis Document Version 1, Sect. 4.2.3.6) to correct continuum pattern that have been observed in spectral fitting residuals. XCO<sub>2</sub>, error metrics and averaging kernels are calculated from the retrieved CO<sub>2</sub> profile following algorithm convergence. Fast cloud screening based on clear-sky surface pressure retrieved from the O<sub>2</sub> A band is applied in the pre-processing to reduce processing overhead on



	<b>ESA Climate Change Initiative (CCI)</b> <b>End-to-end ECV Uncertainty Budget Version 3 (E3UBv3) for the CO2_TAN_OCFP version 1.2 product from the University of Leicester</b> <b>for the Essential Climate Variable (ECV) Greenhouse Gases (GHG)</b>	Page 9
		Version 3
		14 <sup>th</sup> February 2022

unrequired contaminated soundings, whilst a number of post-processing quality filters /Yang et al., 2020/ are applied for removal of low-quality retrievals.

### 5.3 TCCON

The Total Carbon Column Observing Network (TCCON) is a global network of Fourier transform spectrometers built for the purpose of validating space-borne measurements of XCO<sub>2</sub> /Wunch et al., 2010/. TCCON observes these gases with a precision on mole fractions of ~0.15% for CO<sub>2</sub> /Toon et al., 2009/. Although providing highly accurate measurements, the sparseness of the TCCON sites presents a challenge for validation; offering precise GHG measurements for only a limited range of geographic and meteorological conditions.

Additional considerations should be made when validating with TCCON data for the differing sensitivity between TCCON and the satellite instrument, which is partly introduced by different a-priori information used for each retrieval. Removing the influence of the retrieval a-priori, and replacing with the TCCON a-priori could allow for a fairer comparison between the two datasets, but this is not applied here. TCCON data used for error assessments come from the GGG2014 collection (available from <http://tccon.ornl.gov/>).

### 5.4 Co-location

To assess the quality of CO2\_TAN\_OCFP v1 observations against rigorously validated ground based TCCON values, OCFP (TanSat) soundings are matched to TCCON observations spatially and temporally. The process of matching these two data sources is referred to as co-location. Below, we detail the UoL co-location techniques, whose methodology has a bearing on subsequent error statistics.

#### Spatial and Temporal:

OCFP (TanSat) points are co-located with TCCON sites based on a quadrate latitude and longitude region around each TCCON site (in  $\pm 3^\circ$  latitude/longitude box). Matching OCFP soundings with TCCON sites for time is a comparatively simple operation, selecting only those TCCON values whose observation time falls within  $\pm 1$  hour of each OCFP sounding time. The average is taken of all TCCON points fitting these criteria for each OCFP sounding to provide the TCCON value against which to compare.

## 6. Error results

The co-location procedure matches 113,120 points for the CO<sub>2</sub>\_TAN\_OCFP v1 product. As shown in Table 1 and Figure 1, only a small mean overall bias of 0.19 ppm is found, due to the bias correction successfully accounting for most biases at the TCCON sites. An all site Pearson correlation coefficient of 0.82 details a good match of OCFP and TCCON pairs. All-site RMSE (mean of the standard deviation per site) of  $\Delta$  (TCCON- OCFP) is 1.78 ppm.

Site	Mean $\Delta$	$\sigma\Delta$	R	n obs.
Bialystok, Poland	-0.92	1.68	0.65	3,292
Bremen, Germany	0.25	1.20	0.25	1,610
Burgos, Philippines	-0.08	2.22	0.32	310
Darwin, Australia	-0.64	2.05	-0.33	5,534
East Trout Lake, Canada	-0.17	1.26	0.90	11,923
Edwards, USA	-1.40	1.96	0.55	2,763
Garmisch, Germany	-0.32	1.67	0.67	3,704
JPL, USA	1.17	2.07	0.81	15,209
Karlsruhe, Germany	-0.29	1.62	0.84	3,089
Lamont, USA	-0.35	1.35	0.86	18,274
Lauder, New Zealand	-1.31	1.88	0.72	2,999
Orléans, France	-0.66	1.46	0.18	2,243
Paris, France	-0.08	1.40	0.76	1,503
Park Falls, USA	-0.35	1.45	0.89	13,231
Pasadena, USA	1.57	2.47	0.65	12,807
Rikubetsu, Japan	0.54	1.27	0.84	1,473
Sodankylä Finland	-1.18	2.19	0.93	6,482
Saga, Japan	0.69	1.99	0.77	4,033
Tsukuba, Japan	0.94	2.46	0.79	866
Wollongong, Australia	-1.15	1.93	0.73	1,775
<b>Overall</b>	<b>0.19</b>	<b>1.78</b>	<b>0.82</b>	<b>113,120</b>


**Table 1.** Error statistics for all TCCON sites considered for XCO<sub>2</sub> validation. Final row details statistics for all sites, with all co-located points used for calculations. XCO<sub>2</sub> units in ppm. The overall of Mean  $\Delta$  and  $\sigma\Delta$  is calculated by averaging of site value and r is calculated by all individual measurement. Only TCCON measurements over than 20 during each TanSat overpass has been involved in this validation.

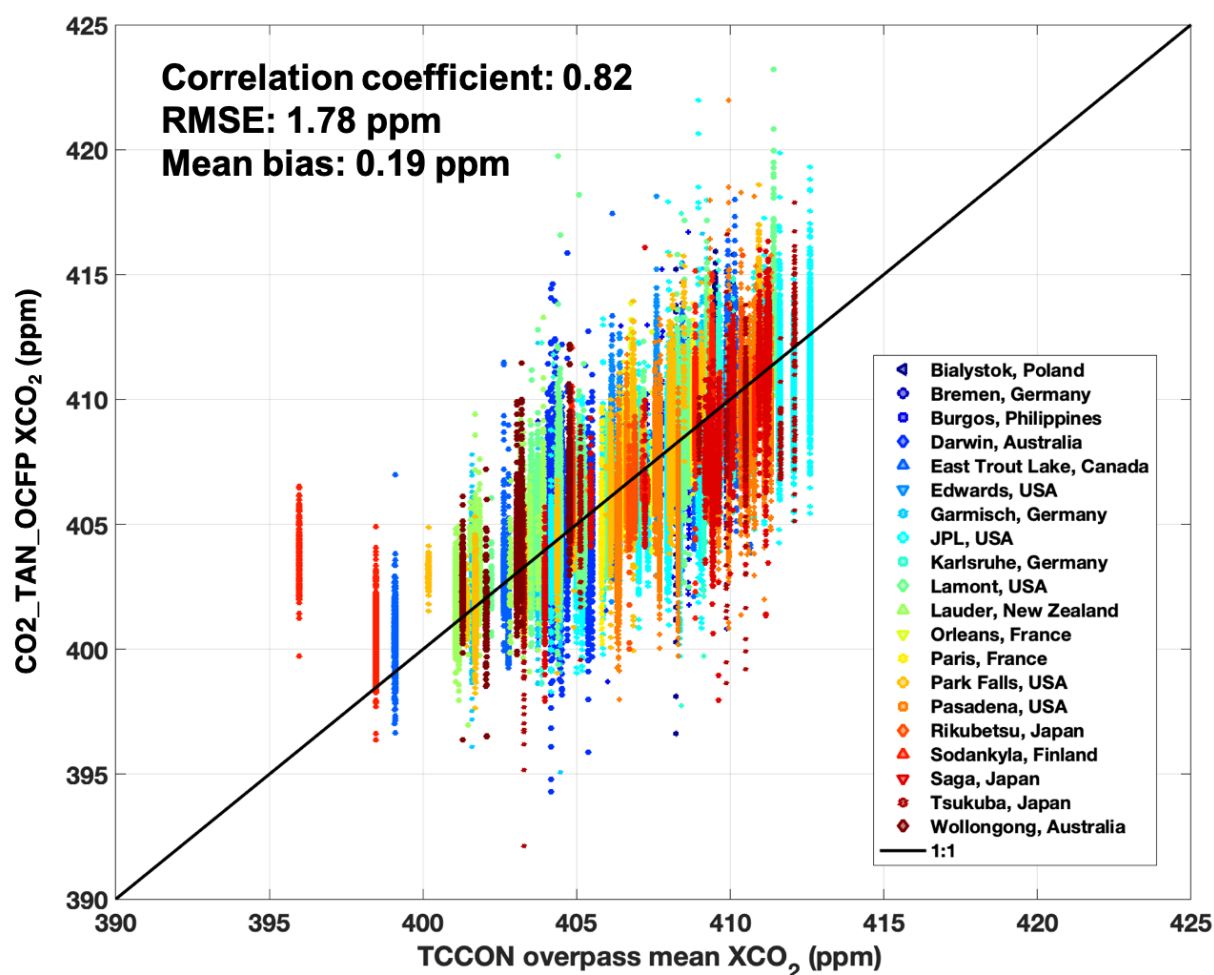
### 6.1 Overview statistics

Figure 2 shows per-site time series of CO<sub>2</sub>\_TAN\_OCFP v1 and TCCON XCO<sub>2</sub>, with mean  $\Delta$ , standard deviation of the  $\Delta$ , correlation coefficient and number of observations shown in Table 1. Filtering of observations and application of a bias correction in post-processing effectively removes significant outliers and for most sites reduces the scatter of OCFP values around the TCCON mean. Note that only measurements for an overpass > 50 soundings are shown in the figure.


### 6.2 Systematic error

Bias correcting reduces the average TCCON–OCFP bias to 0.19 ppm for all sites (Figure 1). As detailed in Figure 2, per-site bias ranges from 1.57 ppm at Pasadena U.S.A., to -1.40 ppm at Edwards, U.S.A. The monthly mean bias for all co-located TCCON–OCFP pairs is shown in Figure 3, and the mean bias per overpass for 8 selected TCCON sites in Figure 4. We define overall systematic error as the standard deviation of inter-site TCCON–OCFP  $\Delta$ , finding a value of 0.84 ppm.

	<b>ESA Climate Change Initiative (CCI)</b> <b>End-to-end ECV Uncertainty Budget Version 3 (E3UBv3) for the CO<sub>2</sub>_TAN_OCFP version 1.2 product from the University of Leicester</b> <b>for the Essential Climate Variable (ECV) Greenhouse Gases (GHG)</b>	Page 11
		Version 3
		14 <sup>th</sup> February 2022



**Figure 1.** Correlation between all 113,120 co-located CO<sub>2</sub>\_TAN\_OCFP and TCCON XCO<sub>2</sub> pairs coloured by site.

	<b>ESA Climate Change Initiative (CCI)</b> <b>End-to-end ECV Uncertainty Budget Version 3 (E3UBv3) for the CO<sub>2</sub>_TAN_OCFP version 1.2 product from the University of Leicester</b> <b>for the Essential Climate Variable (ECV)</b> <b>Greenhouse Gases (GHG)</b>	Page 12
		Version 3
		14 <sup>th</sup> February 2022

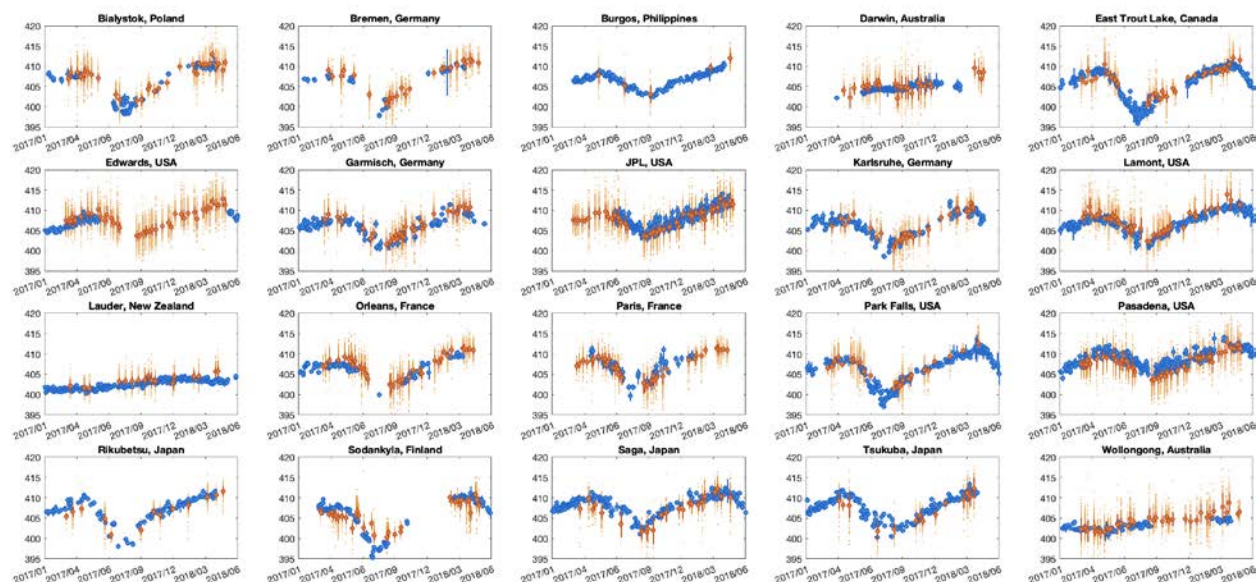


**Figure 2.** TanSat XCO<sub>2</sub> (CO<sub>2</sub>\_TAN\_OCFP v1) observations plotted with their corresponding paired TCCON mean for the overpass. Overview statistics for each site reference to Table 1.

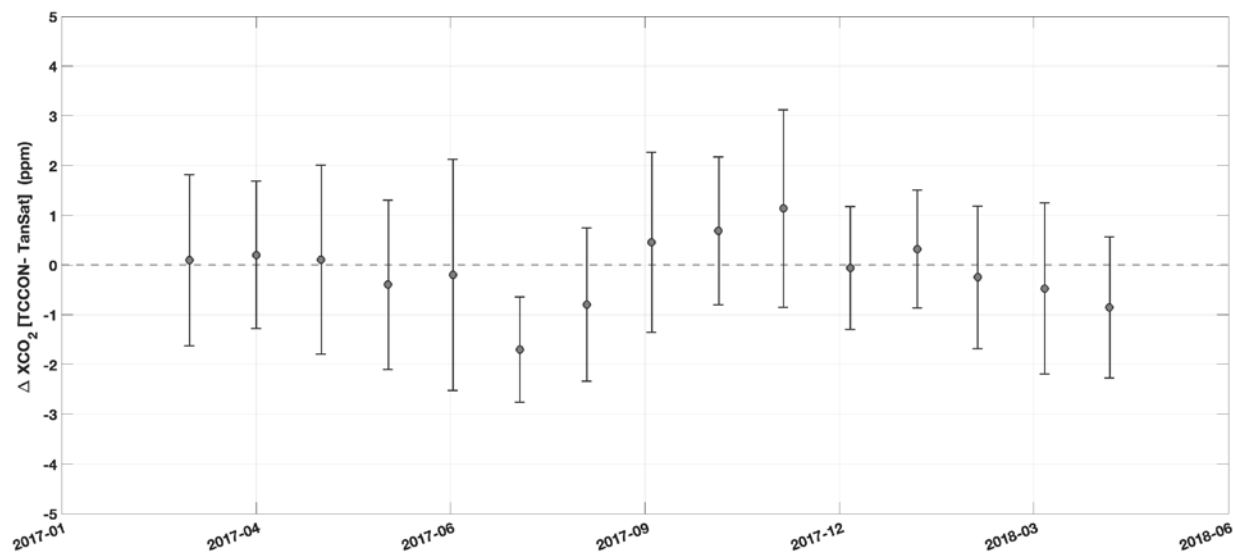


**Figure 3.** Monthly mean OCFP bias against TCCON (all 20 TCCON sites). Vertical error bars represent monthly standard deviation of the bias (the standard deviation of all individual bias).

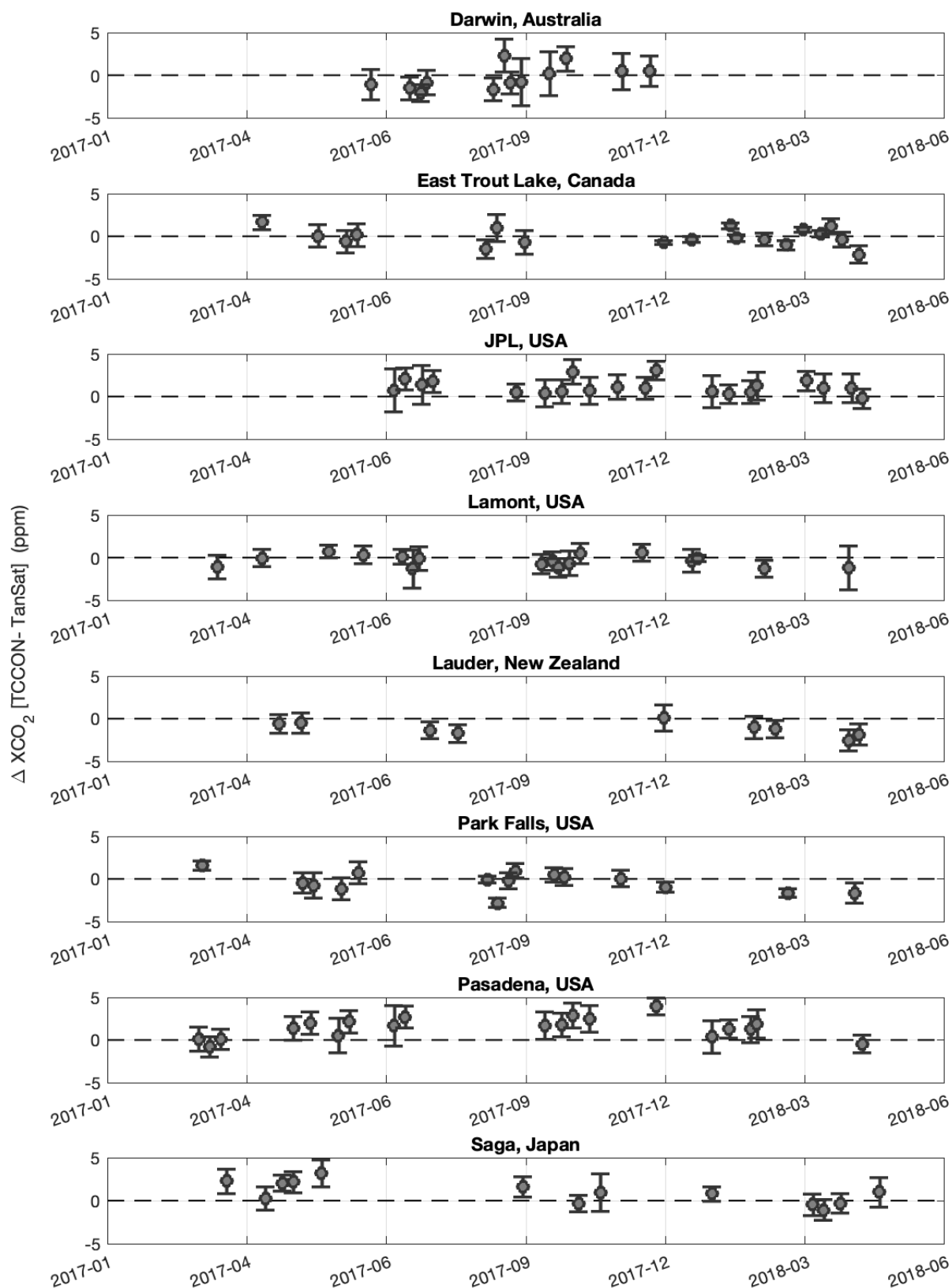


**Figure 4.** Overpass mean of each individual TCCON-OCFP  $\Delta XCO_2$  at 8 TCCON sites. The vertical error bar indicates the standard deviation of individual TCCON-OCFP  $\Delta XCO_2$ .



### 6.3 Correlations

Attempts are made to derive linear dependencies with ancillary OCFP retrieval parameters at all TCCON sites. Here the focus is on total aerosol optical depth, total cirrus optical depth, solar zenith angle (SZA), scale factor of water vapor column and offset of temperature profile. Figure 5 shows the XCO<sub>2</sub> bias against those parameters calculated from all overpass-paired TanSat individual sounding and mean TCCON measurement. Overall, no obvious correlated biased are found with these parameters after the bias correction is applied.

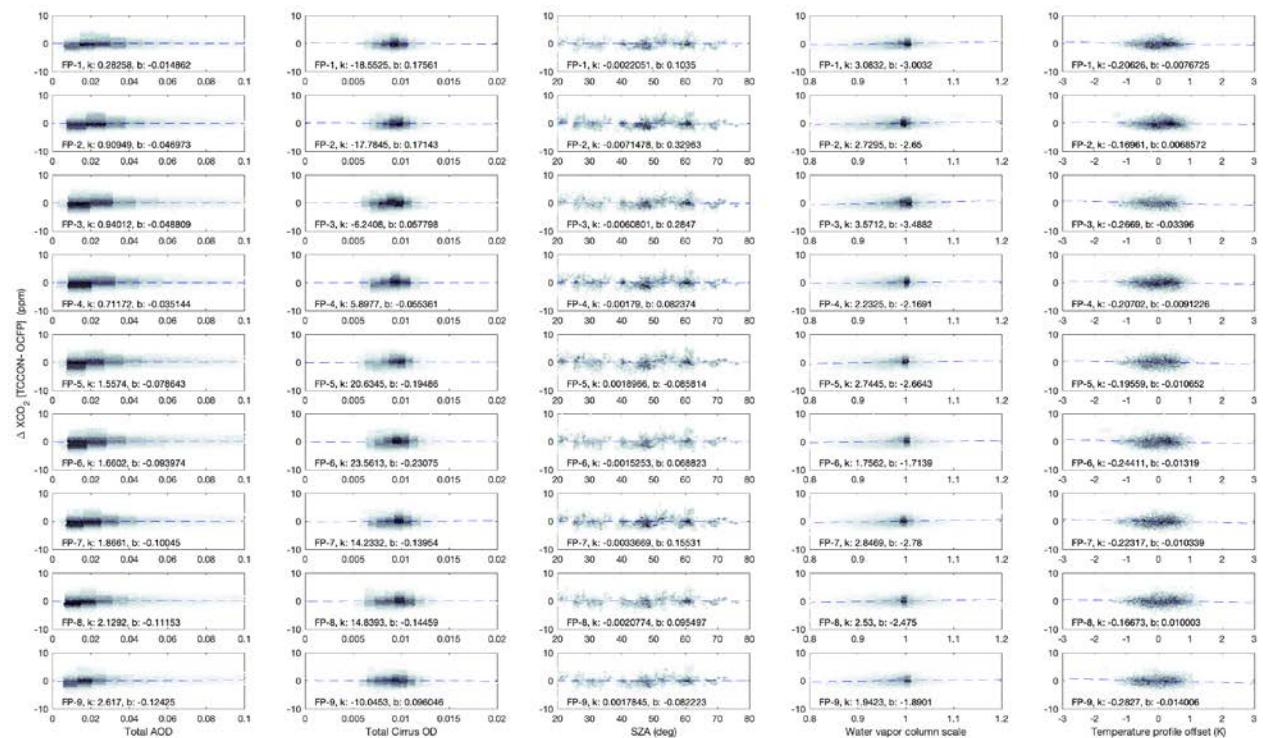



**Figure 5.** XCO<sub>2</sub> bias correlations with total aerosol optical depth, total cirrus optical depth, solar zenith angle (SZA), scale factor of water vapor column and offset of temperature profile (column from left to right) for all co-located TCCON–OCFP pairs. The rows indicate the 9 footprints from top to bottom. The linear regression parameters, slope (k) and offset (b), is shown in each sub-plot.

### 6.4 Random error

The random error is assessed by comparing the overpass-mean product uncertainty at each TCCON site to the standard deviation of the TCCON–OCFP pairs for each overpass and site. Figure 6 shows that the reported uncertainties are between 0.78 ppm (Lamont, U.S.A.) and 4.34 ppm (East Trout Lake, Canada). The correlation plot shows a relatively large spread of the data points which some clear outliers where the observed scatter is largely overestimated. We find that these overestimated errors are correlated with surface albedo of the CO<sub>2</sub> band and these very large a posteriori errors appear when the surface is very dark, and subsequently the SNR is much reduced due to the low level of incident light. In these cases, the information content for CO<sub>2</sub> is limited so that the retrieved results remain close to the a priori values. Thus, they show a low scatter when compared to TCCON resulting in low (0.3 - 1 ppm) values in the mean TCCON–OCFP Δ standard deviation. In future versions, additional quality filters, e.g. continuum level and surface albedo, which correlate with reported a priori errors will be investigated and considered in order to improve posterior errors.

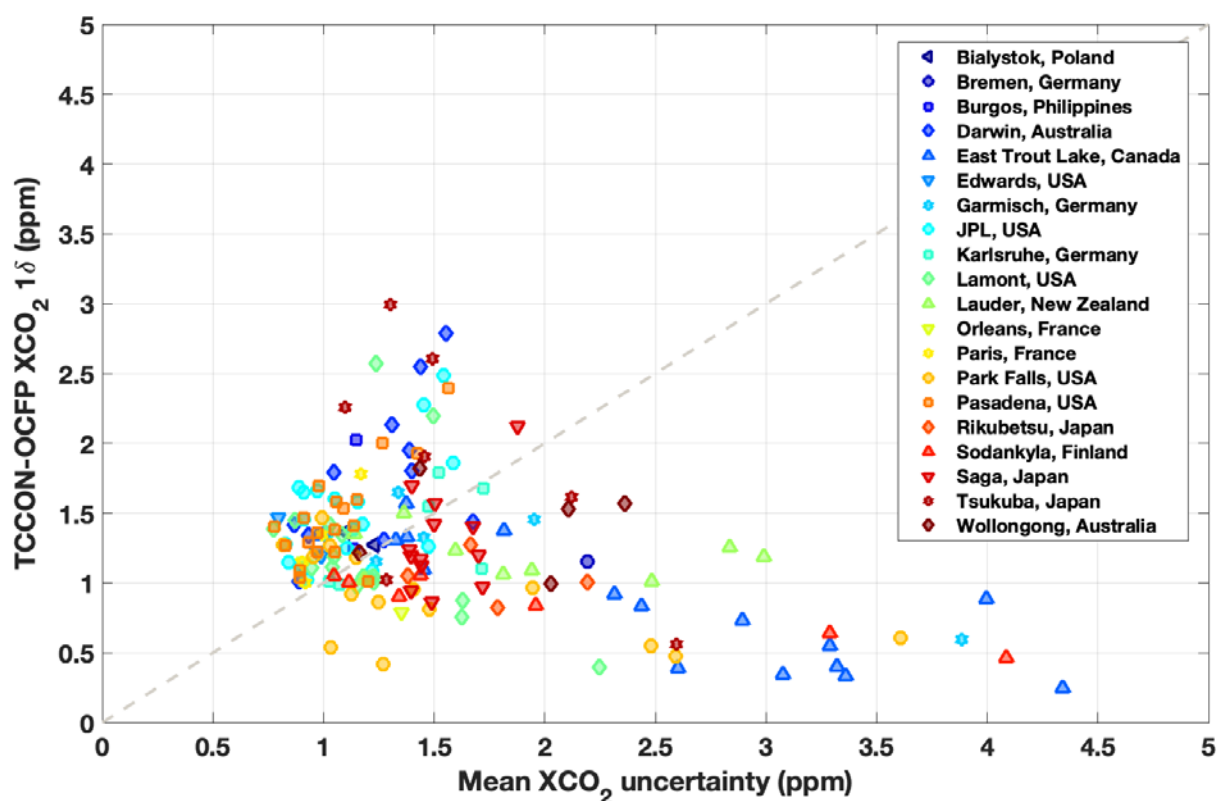



**Figure 6.** Correlation plot of the overpass mean estimate of the a posteriori retrieval error and TCCON-OCFP  $\Delta$  standard deviation for different TCCON sites. Slope and intercept are annotated on plots.

	<b>ESA Climate Change Initiative (CCI)</b> <b>End-to-end ECV Uncertainty Budget Version 3 (E3UBv3) for the CO2_TAN_OCFP version 1.2 product from the University of Leicester</b> <b>for the Essential Climate Variable (ECV) Greenhouse Gases (GHG)</b>	Page 16
		Version 3
		14 <sup>th</sup> February 2022

## 7. Conclusions

From analysis of CO2\_TAN\_OCFP v1 data in conjunction with ground truth data from TCCON we have estimated systematic and random errors, and made some inference towards correlation with external retrieval parameters. A high correlation of the compared CO2\_TAN\_OCFP v1 and TCCON values of 0.82 gives confidence in the retrieval and suggests the post-processing filter and bias correction are working as intended. The random error and systematic error are 1.78 ppm and 0.19 ppm respectively. Stability has not been assessed due to the short time series.




	<b>ESA Climate Change Initiative (CCI)</b> <b>End-to-end ECV Uncertainty Budget Version 3 (E3UBv3) for the CO<sub>2</sub>_TAN_OCFP version 1.2 product from the University of Leicester</b> <b>for the Essential Climate Variable (ECV) Greenhouse Gases (GHG)</b>	Page 17
		Version 3
		14 <sup>th</sup> February 2022

## 8. Acknowledgement

We thank International Reanalysis Cooperation on Carbon Satellites Data (IRCSD) and The Cooperation on the Analysis of carbon Satellites data (CASA) who provided the TanSat L1B data by international collaboration.

## 9. References

- /Boesch et al., 2011/** Boesch, H., Baker, D., Connor, B., Crisp, D. and Miller, C.: Global Characterization of CO<sub>2</sub> Column Retrievals from Shortwave-Infrared Satellite Observations of the Orbiting Carbon Observatory-2 Mission, *Remote Sens.*, 3(12), 270–304, doi:10.3390/rs3020270, 2011.
- /Buchwitz et al., 2011/** Buchwitz, M., Chevallier, F., Bergamaschi, P., Aben, I., Boesch, H., Hasekamp, O., Notholt, J. and Reuter, M.: ESA Green House Gases CCI: User Requirements Document for the GHG-CCI project of ESA's Climate Change Initiative. [online] Available from: [www.esa-ghg-cci.org/?q=webfm\\_send/272](http://www.esa-ghg-cci.org/?q=webfm_send/272) (Accessed 25 January 2016), 2011.
- /Buchwitz et al., 2015/** Buchwitz, M., Reuter, M., Schneising, O., Boesch, H., Guerlet, S., Dils, B., Aben, I., Armante, R., Bergamaschi, P., Blumenstock, T., Bovensmann, H., Brunner, D., Buchmann, B., Burrows, J. P., Butz, A., Chédin, A., Chevallier, F., Crevoisier, C. D., Deutscher, N. M., Frankenberg, C., Hase, F., Hasekamp, O. P., Heymann, J., Kaminski, T., Laeng, A., Lichtenberg, G., De Mazière, M., Noël, S., Notholt, J., Orphal, J., Popp, C., Parker, R., Scholze, M., Sussmann, R., Stiller, G. P., Warneke, T., Zehner, C., Bril, A., Crisp, D., Griffith, D. W. T., Kuze, A., O'Dell, C., Oshchepkov, S., Sherlock, V., Suto, H., Wennberg, P., Wunch, D., Yokota, T. and Yoshida, Y.: The Greenhouse Gas Climate Change Initiative (GHG-CCI): Comparison and quality assessment of near-surface-sensitive satellite-derived CO<sub>2</sub> and CH<sub>4</sub> global data sets, *Remote Sens. Environ.*, 162, 344–362, doi:10.1016/j.rse.2013.04.024, 2015.
- /Chevallier et al., 2014/** Chevallier, F., Palmer, P. I., Feng, L., Boesch, H., O'Dell, C. W. and Bousquet, P.: Toward robust and consistent regional CO<sub>2</sub> flux estimates from in situ and spaceborne measurements of atmospheric CO<sub>2</sub>, *Geophys. Res. Lett.*, 41(3), 1065–1070, doi:10.1002/2013GL058772, 2014.
- /Chen et al., 2012/** Chen, W., Zhang, Y., Yin, Z., Zheng, Y., Yan, C., Yang, Z., and Liu, Y.: The TanSat Mission: Global CO<sub>2</sub> Observation and Monitoring, *Proceedings of the 63rd IAC (International Astronautical Congress)*, Naples, Italy, Oct, IAC-12-B4.4.12, 1-5, 2012.
- /Connor et al., 2008/** Connor, B. J., Boesch, H., Toon, G., Sen, B., Miller, C. and Crisp, D.: Orbiting Carbon Observatory: Inverse method and prospective error analysis, *J. Geophys. Res. Atmospheres*, 113(D5), n/a–n/a, doi:10.1029/2006JD008336, 2008.
- /Liu et al., 2018/** Liu, Y., Wang, J., Yao, L., et al., The TanSat mission: preliminary global observations, *Science Bulletin*, 63, 1200-1207, 2018.
- /Natraj et al., 2008/** Natraj, V., Boesch, H., Spurr, R. J. D. and Yung, Y. L.: Retrieval of X<sub>CO<sub>2</sub></sub> from simulated Orbiting Carbon Observatory measurements using the fast linearized R-2OS radiative transfer model, *J. Geophys. Res.*, 113(D11), doi:10.1029/2007JD009017, 2008.
- /O'Dell et al., 2010/** O'Dell, C. W.: Acceleration of multiple-scattering, hyperspectral radiative transfer calculations via low-streams interpolation, *J. Geophys. Res.*, 115(D10), doi:10.1029/2009JD012803, 2010.
- /Toon et al., 2009/** Toon, G., Blavier, J.-F., Washenfelder, R., Wunch, D., Keppel-Aleks, G., Wennberg, P., Connor, B., Sherlock, V., Griffith, D., Deutscher, N. and Notholt, J.: Total Column Carbon Observing Network (TCCON), p. JMA3, OSA., 2009.
- /Wagner et al., 2012/** Wagner, W., Dorigo, W., de Jeu, R., Parinussa, R., Scarrott, R., Kimmo, Lahoz, W., Doubková, M., Dwyer, N. and Barrett, B.: ESA Soil Moisture CCI: Comprehensive Error Characterisation Report. [online] Available from: <http://www.esa-soilmoisture-cci.org/sites/default/files/documents/public/Deliverables%20>

	<b>ESA Climate Change Initiative (CCI)</b> <b>End-to-end ECV Uncertainty Budget Version 3 (E3UBv3) for the CO2_TAN_OCFP version 1.2 product from the University of Leicester</b> <b>for the Essential Climate Variable (ECV) Greenhouse Gases (GHG)</b>	Page 18
		Version 3
		14 <sup>th</sup> February 2022

%20CCI%20SM%201/20120521\_CCI\_Soil\_Moisture\_D1.2.1\_CECR\_v.0.7.pdf (Accessed 25th January 2016), 2012.

**/Wunch et al., 2010/** Wunch, D., Toon, G. C., Wennberg, P. O., Wofsy, S. C., Stephens, B. B., Fischer, M. L., Uchino, O., Abshire, J. B., Bernath, P., Biraud, S. C., Blavier, J.-F. L., Boone, C., Bowman, K. P., Browell, E. V., Campos, T., Connor, B. J., Daube, B. C., Deutscher, N. M., Diao, M., Elkins, J. W., Gerbig, C., Gottlieb, E., Griffith, D. W. T., Hurst, D. F., Jiménez, R., Keppel-Aleks, G., Kort, E. A., Macatangay, R., Machida, T., Matsueda, H., Moore, F., Morino, I., Park, S., Robinson, J., Roehl, C. M., Sawa, Y., Sherlock, V., Sweeney, C., Tanaka, T. and Zondlo, M. A.: Calibration of the Total Carbon Column Observing Network using aircraft profile data, *Atmospheric Meas. Tech.*, 3(5), 1351–1362, doi:10.5194/amt-3-1351-2010, 2010.

**/Yang et al., 2018/** Yang, D., Y. Liu, Z. Cai, X. Chen, L. Yao, and D. Lu, 2018: First Global Carbon Dioxide Maps Produced from TanSat Measurements. *Adv. Atmos. Sci.*, 35(6), 621–623.

**/Yang et al., 2020/** Yang, D. Boesch, H., Liu, Y., Somkuti, P., et al.: Toward high precision XCO<sub>2</sub> retrieval on TanSat measurements: the retrieval improvement and validation against TCCON measurement. *J. Geophys. Res. Atmos.*, 2020, 125, e2020JD032794.